Theory of Self-Trapped Exciton Luminescence in Halide Crystals*

W. Beall Fowler
Department of Physics, Lehigh University, Bethlehem, Pennsylvania 18015

M. J. Marrone and M. N. Kabler
Naval Research Laboratory, Washington, D. C. 20375

(Received 30 July 1973)

A detailed phenomenological theory of the triplet luminescence from self-trapped excitons in halide crystals is developed. Energy levels and wave functions are obtained by constructing and diagonalizing a Hamiltonian matrix. Coupled rate equations for the decay of the three lowest triplet levels are solved for the general case in which the levels are not in thermal equilibrium, and circular polarizations, light intensities, and excited-state lifetimes are obtained as functions of temperature, magnetic field, and crystal orientation. KI and CsI excitons are used as detailed examples; the latter is of particular interest because it appears to exhibit a level crossing at $\sim$45 kG. The theory is also appropriate to other systems, including the excited M center and the relaxed excited Tl^+ ion in alkali halides.

I. INTRODUCTION

A number of atomic, molecular, and solid-state systems involve the electronic configurations (p^5s) and (sp). For example, the lowest excited states of Tl^+-like ions[1] are (in the absence of configuration interaction) derived from Tl^+ $6s\,6p$. When Tl^+ is in a crystal, the symmetry is lowered and additional splittings and mixings occur. Other configurations may also become important, but in zeroth order a number of effects are described as occurring within the $6s\,6p$ configuration.

Excitons in rare-gas solids and in alkali halides[2] may be approximately constructed from a p^5s configuration on the rare-gas atom (or halogen), suitably modified to take into account crystal effects. It is found that at low temperatures these excitons may become self-trapped[3] into a molecular-type species. In the case of the alkali halides, this self-trapped exciton (STE) may also be regarded as a V_K center plus an electron. This is still an excited state, which may decay to the ground state either radiatively or nonradiatively.

Considerable experimental work has been performed, in both luminescence and absorption, on the systems mentioned.[1,4-6] Some of this work has involved the measurement of circular dichroisms or radiative-lifetime changes in external magnetic fields. In this paper we develop a simple phenomenological approach to calculate energies and wave functions as a function of magnetic field. Coupled rate equations for the decay of the three lowest STE triplet levels are solved for the general case in which the levels are not in thermal equilibrium, and light intensities, excited-state lifetimes, and circular polarizations are obtained as functions of temperature, magnetic field, and crystal orientation. Self-trapped excitons in KI and CsI are treated as examples. Some preliminary results of this work have been reported elsewhere.[7]

II. THEORY

A. Atom in a Crystal Field

We shall consider first an sp or p^5s atom in a crystal field,[8,9] in an applied static magnetic field. Later we shall indicate how these results may be generalized to treat molecular systems.

The wave-function basis consists of 12 components. We choose quantization directions X, Y, Z for the orbital p functions such that, in the static lattice, the crystal field does not mix them, i.e., we assume orthorhombic or higher symmetry. We also neglect vibrational effects. It is assumed that the crystal field may lift the spatial degeneracy of these states, hence a further reduction (e.g., to a single 4×4) is not possible, in general.

The problem may be simplified somewhat, however, by a careful choice of basis, namely, linear combinations of space and spin functions to form singlets and triplets. Explicitly, this basis is as follows: Let $\psi_s(\vec{r})$, $\psi_i(\vec{r})$ be one-electron s- and p-like functions, where $i=x$, y, or z. α (up) and β (down) are spin functions.[10]

These space and spin functions are first combined into the following form:

$$\begin{aligned}
\varphi_i^1 &= 2^{-1/2}[\psi_s(\vec{r}_1)\psi_i(\vec{r}_2)-\psi_i(\vec{r}_1)\psi_s(\vec{r}_2)]\,,\\
\varphi_i^2 &= 2^{-1/2}[\psi_s(\vec{r}_1)\psi_i(\vec{r}_2)+\psi_i(\vec{r}_1)\psi_s(\vec{r}_2)]\,,\\
\chi_1 &= 2^{-1/2}[\alpha(1)\alpha(2)+\beta(1)\beta(2)]\,,\\
\chi_2 &= 2^{-1/2}[\alpha(1)\beta(2)+\beta(1)\alpha(2)]\,,\\
\chi_3 &= 2^{-1/2}[\alpha(1)\alpha(2)-\beta(1)\beta(2)]\,,\\
\chi_4 &= 2^{-1/2}[\alpha(1)\beta(2)-\beta(1)\alpha(2)]\,,
\end{aligned} \tag{1}$$

and the basis functions then are

$$^3X_1=\varphi_x^1\chi_1\,,\quad ^3Y_1=\varphi_y^1\chi_1\,,\quad ^3Z_1=\varphi_z^1\chi_1\,,$$
$$^3X_2=\varphi_x^1\chi_2\,,\quad ^3Y_2=\varphi_y^1\chi_2\,,\quad ^3Z_2=\varphi_z^1\chi_2\,,$$

$$^3X_3=\varphi_x^1\chi_3\,,\quad ^3Y_3=\varphi_y^1\chi_3\,,\quad ^3Z_3=\varphi_z^1\chi_3\,, \tag{2}$$
$$^1X=\varphi_x^2\chi_4\,,\quad ^1Y=\varphi_y^2\chi_4\,,\quad ^1Z=\varphi_z^2\chi_4\,.$$

In terms of these functions one can then construct a complete Hamiltonian matrix. By choosing them as singlets and triplets, the states are already diagonal with respect to exchange. Since the crystal field acts only to split X, Y, Z, and not to mix them, the matrix would also be diagonal in crystal field. The matrix is not, however, diagonal with respect to magnetic interactions, in particular, spin-orbit and Zeeman interactions. Thus off-diagonal matrix elements must be calculated.

The system Hamiltonian (as applied to the above basis) is written as

$$\mathcal{H}=\sum_{k=1}^{2}[p_k^2/2m+U(\vec{r}_k)+\zeta(r_k)\vec{l}_k\cdot\vec{s}_k + \mu_B(\vec{l}_k+2\vec{s}_k)\cdot\vec{H}\,]+e^2/r_{12}\,. \tag{3}$$

Here the second term $U(\vec{r}_k)$ is a one-electron operator containing atomic, molecular, and crystal-field interactions. The third term is the spin-orbit interaction and the fourth term is the Zeeman interaction. μ_B is the Bohr magneton $e/2mc$. The first, second, and fifth terms are diagonal with respect to our basis, while the third and fourth terms are off diagonal. By systematically evaluating the matrix elements of these operators with respect to the basis, we obtain the 12×12 Hamiltonian matrix shown in Table I.

The symbols appearing in Table I have the following meanings: A, B, C, D, E, F are diagonal elements of the various singlet and triplet X, Y, and Z states, as indicated. Crystal-field and exchange effects are implicitly included in these terms. H_x, H_y, H_z are the spatial components of the applied magnetic field. G is a spin-orbit parameter which is given by

$$G=\pm\tfrac{1}{2}\langle R_i(r)\,|\,\zeta(r)\,|R_j(r)\rangle\,,\quad i\neq j \tag{4}$$

where the R_i's are radial parts of the one-electron ψ_i's and the angular brackets represent integrals over the r coordinate. The sign of G is positive for (sp), negative for (p^5s). In the case of atoms the bracket of Eq. (4) is equal to the quantity ζ defined by Condon and Shortley.[8] δ and δ' are parameters whose meaning will be discussed later; for atoms each is equal to 1.

The Hamiltonian matrix (Table I) has been arranged so as to emphasize the nature of the zero-field states and to indicate the nature of the magnetic field coupling. In the absence of a magnetic field the matrix reduces to four (uncoupled) 3×3's, all of similar structure. As may be seen, three of these involve two triplets and a singlet, while the fourth involves only triplet states. Thus in

TABLE I. Hamiltonian matrix for the STE and similar systems. Parameters are defined in the text. Basis functions are indicated; in some cases they have been multiplied by factors of $(\pm1$ or $\pm i)$ in order to emphasize similarities in the matrix.

	$^3Z_1$	^1X	$(-i)^3Y_2$	$^3Z_2$	$(-)^3X_3$	$(-i)^3Y_1$	$^3Z_3$	$^3X_2$	$(-i)^1Y$	^1Z	$(-)^3X_1$	$(-i)^3Y_3$
$^3Z_1^*$	A	$-G\delta'$	$G\delta'$	$2\mu_BH_x$	0	$\delta\mu_BH_x$	$2\mu_BH_z$	0	0	0	$i\delta\mu_BH_y$	0
$^1X^*$	$-G\delta'$	D	G	0	0	0	0	0	$-\mu_BH_z$	$i\delta\mu_BH_y$	0	0
$(i)^3Y_2^*$	$G\delta'$	G	E	$\delta\mu_BH_x$	0	$2\mu_BH_x$	0	$-\mu_BH_z$	0	0	0	$2i\mu_BH_y$
$^3Z_2^*$	$2\mu_BH_x$	0	$\delta\mu_BH_x$	A	$-G\delta'$	$G\delta'$	$2i\mu_BH_y$	$-i\delta\mu_BH_y$	0	0	0	0
$(-)^3X_3^*$	0	0	0	$-G\delta'$	C	G	$-i\delta\mu_BH_y$	$2i\mu_BH_y$	0	0	$2\mu_BH_z$	μ_BH_z
$(i)^3Y_1^*$	$\delta\mu_BH_x$	0	$2\mu_BH_x$	$G\delta'$	G	E	0	0	0	0	μ_BH_z	$2\mu_BH_z$
$^3Z_3^*$	$2\mu_BH_z$	0	0	$-2i\mu_BH_y$	$i\delta\mu_BH_y$	0	A	$-G\delta'$	$G\delta'$	0	0	$\delta\mu_BH_x$
$^3X_2^*$	0	0	$-\mu_BH_z$	$i\delta\mu_BH_y$	$-2i\mu_BH_y$	0	$-G\delta'$	C	G	0	$-2\mu_BH_x$	0
$(i)^1Y^*$	0	$-\mu_BH_z$	0	0	0	0	$G\delta'$	G	F	$\delta\mu_BH_x$	0	0
$^1Z^*$	0	$-i\delta\mu_BH_y$	0	0	0	0	0	0	$\delta\mu_BH_x$	B	$-G\delta'$	$G\delta'$
$(-)^3X_1^*$	$-i\delta\mu_BH_y$	0	0	0	$2\mu_BH_z$	μ_BH_z	0	$-2\mu_BH_x$	0	$-G\delta'$	C	G
$(i)^3Y_3^*$	0	0	$-2i\mu_BH_y$	0	μ_BH_z	$2\mu_BH_z$	$\delta\mu_BH_x$	0	0	$G\delta'$	G	E

the absence of magnetic fields and other perturbations there will be three pure-triplet states, while all the rest will involve admixtures of singlet and triplet.

Given values of the various quantities included in Table I, one may then diagonalize the matrix and obtain the 12 eigenvalues and the 12 wave-function coefficients for each eigenvalue. In cases of interest optical transitions involve a lower ^1S state, and so various transition parameters (dichroisms, lifetimes, etc.) will depend on the admixture of ^1X, ^1Y, ^1Z in the various excited states.

B. Molecular Systems

We now generalize the preceding to a diatomic system whose axis is chosen to be z. A molecular analog of (sp) would, for example, be an excited hydrogen molecule or an excited M center, while the molecular analog of (p^5s) is the STE. Such systems possess two equivalent centers (if the site has inversion symmetry), which means that a wave function constructed from atomic orbitals will involve overlapping contributions from both centers. More fundamentally, there will in general be twice as many states as in the case of one atom. These states may be classified as odd (u) or even (g) under inversion through the molecular center, and since the u and g states do not interact with each other, one may treat each class separately. Thus, in effect, one still has a 12×12 problem to solve.

The structure of this molecular 12×12 is essentially the same as that discussed in Sec. II A, with some differences in detail. The problem is set up in the same general way, except that now the functions $\psi_i(r)$ are not atomic p functions but are molecular orbitals[11] of either axial (Z) or transverse $(X$ or $Y)$ symmetry. These might, for example, be constructed from atomic orbitals centered on the atoms, but this detail is not important at present.

It is important, however, to recognize how the matrix elements of $\mathcal{H}$ may be different from the atomic case. In general there will be numerical differences, e.g., in diagonal elements, but in addition there may be systematic differences.[12] We expect in particular that matrix elements involving the angular momentum operator will be systematically changed and will depend upon whether one is coupling X to Y, or Z to X or Y. The reason for this is that the Z (Σ-like) state will differ considerably from X or Y (Π-like) states. For the STE the Z state will involve a σ_u-type hole molecular orbital (MO), while the X and Y states will involve π_u-type hole MO's. If, for example, one were to construct these MO's from atomic orbitals, one would find different normalization factors due to different overlaps in the σ and π cases. Consequently, although the angular momentum operating on Z may generate a function of symmetry X or Y, that function will not be identical to the X or Y basis and so will not have unit matrix element with the basis. These comments are also valid when applied to X vs Y, but since these are both Π states and therefore rather similar in nature, we assume that the angular momentum matrix elements involving them are as in the atomic case.

We take account of this distinction in angular momentum matrix elements by introducing angular momentum multiplication factors δ and δ'. They have been included in Table I but were chosen equal to 1 for atoms. Note that δ' occurs in spin-orbit terms, and δ in orbital Zeeman terms which couple Z to X or Y.

The Hamiltonian matrix has, then, been determined for the diatomic analog of a p^5s or sp system. It contains nine distinct parameters, each of which could be calculated as part of a detailed theory of the system. We have not developed such a theory, but will show that reasonable estimates of all of these quantities are obtainable from other types of experiments. In Sec. II C we discuss how these parameters may be obtained for the STE in alkali halides.

C. Determination of Hamiltonian Parameters for the STE

The choice of one diagonal parameter merely amounts to rigidly shifting the excited-state array in energy, without changing the internal structure of the 12 states. Consequently, the zero-order ^3Z energy A is arbitrarily set equal to zero. The other diagonal elements are $B(^1Z)$, $C(^3X)$, $D(^1X)$, $E(^3Y)$, and $F(^1Y)$. For each of Z, X, Y, the triplet-singlet energy difference is an exchange energy. This energy has been estimated for the unrelaxed exciton,[13,14] but there is experimental evidence[15] that in some cases the exchange parameter for the STE is more than an order of magnitude smaller than values reported for the unrelaxed exciton in Ref. 13. The only systems considered in detail here are ones for which some experimental evidence exists regarding the STE exchange parameter.

Two more diagonal parameters remain: ^3X and ^3Y. The off-diagonal parameters G, δ, δ' must also be obtained. The spin-orbit parameter G may also be estimated from the optical-absorption spectrum.[13] In most cases values so obtained vary but slightly from those reported in Ref. 16. δ, δ', ^3X, and ^3Y may be estimated from an analysis of the electron-spin-resonance[16] properties of the V_K center, a self-trapped hole in a σ_u-like orbital. The STE is created when a V_K traps an electron into a symmetric ($\approx s$-like) orbital, and there is thus a direct correspondence between the energy

TABLE II. Hamiltonian matrix for V_K. Parameters are defined in the text.

	$(Z\alpha)$	$(Z\beta)$	$(X\alpha)$	$(X\beta)$	$(Y\alpha)$	$(Y\beta)$
$(Z\alpha)^*$	$A+\mu_B H_z$	$\mu_B(H_x-iH_y)$	$-i\delta\mu_B H_y$	$-\delta' G$	$i\delta\mu_B H_x$	$i\delta' G$
$(Z\beta)^*$	$\mu_B(H_x+iH_y)$	$A-\mu_B H_z$	$\delta' G$	$-i\delta\mu_B H_y$	$i\delta' G$	$i\delta\mu_B H_x$
$(X\alpha)^*$	$i\delta\mu_B H_y$	$\delta' G$	$C+\mu_B H_z$	$\mu_B(H_x-iH_y)$	$-iG-i\mu_B H_z$	0
$(X\beta)^*$	$-\delta' G$	$i\delta\mu_B H_y$	$\mu_B(H_x+iH_y)$	$C-\mu_B H_z$	0	$iG-i\mu_B H_z$
$(Y\alpha)^*$	$-i\delta\mu_B H_x$	$-i\delta' G$	$iG+i\mu_B H_z$	0	$E+\mu_B H_z$	$\mu_B(H_x-iH_y)$
$(Y\beta)^*$	$-i\delta' G$	$-i\delta\mu_B H_x$	0	$-iG+i\mu_B H_z$	$\mu_B(H_x+iH_y)$	$E-\mu_B H_z$

levels and hole wave functions of the V_K and those of the STE.

This relationship may be exhibited quite clearly if one constructs a V_K energy matrix using the same type of analysis as used in constructing Table I. This will only be a 6×6, but the basis functions will be products of spin functions and σ- and π-type hole MO's. Hamiltonian operators include crystal field, spin-orbit, and Zeeman terms, and consequently the V_K matrix consists of some of the same types of elements as given in Table I. Table II illustrates a Hamiltonian matrix for the V_K center.

The triplet energies C and E and the orbital multiplication factors δ and δ' are determined by using experimental values of the g factors g_x, g_y, and g_z for the V_K center. These are related to the level spectrum as follows: For $H_x=H_y=0$, the splitting between the two lowest energy states will vary approximately linearly with H_z, with a slope of $g_z\mu_B$. A similar procedure yields g_x and g_y. One may vary the parameters until satisfactory agreement with experimental values is obtained.[17]

In fact, such analyses have been performed on the V_K center using perturbation theory. Castner and Känzig[18] obtained the first data on V_K centers and analyzed them along these lines. More recently, Schoemaker[16] has obtained more precise experimental values of the g factors for a number of centers. His analysis includes numerical estimates of the parameters δ and δ', and since the perturbation results vary only slightly from those which we have obtained by exact diagonalization, we simply use the values of δ, δ', C, E (and G) with which Schoemaker fitted his data. It should be noted that these values of C and E are consistent with STE absorption data.[19] At this stage of the analysis, all of the energy parameters may be tentatively determined and are given in Table III for a number of alkali halides. Only KI and CsI are treated in detail in this paper.

D. Calculation of Energies and Wave Functions

Since the STE Hamiltonian matrix is now determined as a function of magnetic field, energy levels and wave functions may be obtained. The transition probability and polarization for a given magnitude and direction of H, a given center orientation, and a given direction of observation, will depend upon the occupancy of the levels and the fraction of particular singlet wave function in those levels.

TABLE III. Parameters for use in the STE calculation. Definitions are given in the text. With the exception of all CsI parameters and of the exchange parameters (B), all values were based upon Schoemaker, Ref. 16. The value of B for CsI was chosen to fit data; other CsI values were inferred from KI values. The value of B for KI is from Petroff *et al.*, Ref. 14 and that in parenthesis for KBr is from Kabler *et al.*, Ref. 15. Values of B for the other substances are from the papers cited in Ref. 13, and should be taken with some caution in application to the STE.

	(eV)						
Crystal	A	B	C	E	G	δ	δ'
NaCl	0	0.048	2.452	2.108	0.033	0.72	1.07
KCl	0	0.053	2.360	2.480	0.033	0.73	1.07
RbCl	0	0.058	2.264	2.616	0.033	0.75	1.07
NaBr	0	0.37	2.162	1.738	0.140	0.69	1.07
KBr	0	0.26(0.0076)	2.1865	2.1935	0.140	0.70	1.07
RbBr	0	0.16	2.132	2.328	0.140	0.70	1.07
KI	0	0.044	2.015	2.045	0.292	0.70	1.07
CsI	0	0.035	2.1	2.1	0.292	0.70	1.07

The results, in detail, will depend upon the orientation of the STE with respect to magnetic field and observation direction. For CsI and CsBr experiments were performed on crystals oriented in both [001] and [111] directions. In the former case, the possible STE orientations include one parallel and two perpendicular to the field, while in the latter case all centers make an angle of $\cos^{-1}\sqrt{\frac{1}{3}}$ with the field.

In the fcc alkali halides, experiments of the type analyzed in this paper were performed on [001] crystals.[5] In this case, four center orientations are equivalent to [101] and two to [110] with respect to the field. Experimental constraints have required that the luminescence be observed along the direction parallel to the field.

Assuming that all orientations are equally populated, the next part of the calculation for each center is to include the H-field components with respect to the coordinates within the center. After the matrix is solved and wave functions are obtained, one then projects the wave-function coefficients into the "laboratory" coordinates in which $\vec{H} = H_z$.

As an example, consider a center in the fcc lattice aligned along [101]. We define quantization axes within the center as x', y', z', with unit vectors $\hat{i}_{x'} = \sqrt{\frac{1}{2}}(1,0,\bar{1})$, $\hat{i}_{y'} = (0,1,0)$, $\hat{i}_{z'} = \sqrt{\frac{1}{2}}(1,0,1)$. These primed axes correspond to the axes defined in the energy matrix. This notation is consistent with that of Ref. 18, but x' and y' are opposite to those of Ref. 16. The magnetic field then has components

$$H_{x'} = -\sqrt{\tfrac{1}{2}} H_{\text{applied}} ,$$
$$H_{z'} = \sqrt{\tfrac{1}{2}} H_{\text{applied}} . \tag{5}$$

Diagonalization will yield coefficients of singlet wave function in x', y', z' directions; call these $C_{x'}$, $C_{y'}$, $C_{z'}$. The total radiative transition probability from a given state will be proportional to the quantity $C_{x'}^* C_{x'} + C_{y'}^* C_{y'} + C_{z'}^* C_{z'}$. To compute circular polarization of light emitted along the z axis, one first projects these coefficients back into the (xy) plane:

$$C_x = \sqrt{\tfrac{1}{2}}(C_{x'} + C_{z'}) , \quad C_y = C_{y'} ; \tag{6}$$

one then forms $C_x + iC_y$, $C_x - iC_y$, and defines

$$I_+ \propto (C_x + iC_y)(C_x^* - iC_y^*) ,$$
$$I_- \propto (C_x - iC_y)(C_x^* + iC_y^*) . \tag{7}$$

The circular polarization, if only this level and this center emitted light, would equal $(I_+ - I_-)/(I_+ + I_-)$.

For the center aligned along [110] a similar (but simpler) analysis may be applied, and for the cesium chloride lattice similar results are also obtained. At this stage of the calculation one has energy levels, and for each level of each center one has a number representing each of I_+, I_-, and I_z. The last quantity represents light emitted with dipole parallel to H; this light will not be detected for an observation direction along H.

E. Rate Equations

As will be indicated in Sec. III, there is strong evidence in a number of instances that the triplet levels are not in thermal equilibrium. Consequently, one must solve three coupled rate equations which involve both radiative and nonradiative decay times. These equations may be written in the form

$$\frac{dn_i}{dt} = \sum_{j=1}^{3} C_{ij} n_j , \tag{8}$$

where n_i is the probability at time t that level i is occupied. The rate constants C_{ij} are obtained from the various mechanisms for populating and depopulating levels. Nonradiative decays are assumed to occur via one-phonon "direct" processes,[20] in which an energy-conserving phonon is either emitted or absorbed, and via no-phonon tunneling processes.[21] The latter are important only when two levels are nearly degenerate. Recent considerations[15] suggest that high-order hyperfine interactions may lead to mixing of nearly degenerate levels. This mixing would change radiative decay probabilities of such levels, and would have much the same effect as the tunneling processes considered here, namely, the depopulation of long-lived states. It should be noted that in our treatment Orbach processes[22] are included in the direct matrix elements through the coupled rate equations.

As examples, expressions for three of the rate constants are

$$C_{11} = -\frac{1}{\tau_{1R}} - \frac{1}{\tau_{12}}\bar{n}_{12} - \frac{1}{\tau_{13}}\bar{n}_{13} - \frac{1}{\tau_T} \times e^{-A_T(E_2 - E_1)} - \frac{1}{\tau_T} e^{-A_T(E_3 - E_1)} ,$$
$$C_{21} = \frac{1}{\tau_{12}}\bar{n}_{12} + \frac{1}{\tau_T} e^{-A_T(E_2 - E_1)} \tag{9}$$
$$C_{12} = \frac{1}{\tau_{12}}(\bar{n}_{12} + 1) + \frac{1}{\tau_T} e^{-A_T(E_2 - E_1)} .$$

The other constants are similarly obtained. In Eq. (9), τ_T and A_T are parameters related to the nonradiative tunneling. τ_{ij}^{-1} is related to the one-phonon tunneling and is taken, for reasons discussed in Sec. III B, to be proportional to $|E_j - E_i|^2$. $\bar{n}_{ij}$ is the Planck function

$$\bar{n}_{ij} = \frac{1}{e^{(E_j - E_i)/kT} - 1} . \tag{10}$$

τ_{iR}^{-1} is the radiative-decay probability from state i.

Solution of Eq. (8) is obtained by writing each n_i as the sum of three terms of the form

$$n_i = \sum_{j=1}^{3} D_{ij} e^{-m_j t}. \tag{11}$$

Substitution of Eq. (11) into Eq. (8) leads to simultaneous linear equations which can be solved to yield each D_{ij} and m_j. The measured decay times correspond to the quantities m_j^{-1}.

The amount of decay that is radiative, n_{iR}, is obtained for each level by integrating Eq. (8) over time, including only those parts of C_{ij} corresponding to radiative decay, i.e., the quantities $-1/\tau_{iR}$ in C_{ii}. The final steps, computing circular polarizations and intensities, involve the quantities n_{iR} and the intensities $I_+(i)$, $I_-(i)$, $I_z(i)$ introduced in Sec. II D. Namely, for each center the circular polarization P is

$$P = \sum_i n_{iR} \frac{I_+(i) - I_-(i)}{I_+(i) + I_-(i) + I_z(i)} \tag{12}$$

and the intensity which will be observed is

$$\mathcal{I} = \sum_i n_{iR} \frac{I_+(i) + I_-(i)}{I_+(i) + I_-(i) + I_z(i)} . \tag{13}$$

One then combines results for the different orientations of centers in a crystal to predict observed quantities; the fractional circular polarization is given by the sum of the P's [Eq. (12)] divided by the sum of the $\mathcal{I}$'s [Eq. (13)].

F. Discussion of Theory

Before proceeding to detailed application of the theory, it is instructive to discuss some aspects of it. Many of the results to be presented may be understood qualitatively by perturbation analyses of the energy matrix, Table I. We consider first the zero-field splittings of the three lowest triplet levels, denoted as ${}^3Z$. Each of these mixes with two higher levels, as indicated in the diagonal blocks. The level denoted as ${}^3Z_2$ mixes only with other triplets; its energy will be given approximately by

$$E_{A_u} = A - G^2\delta'^2\left(\frac{1}{C-A} + \frac{1}{E-A} - \frac{2|G|}{(C-A)(E-A)}\right). \tag{14}$$

The other two levels will each have some singlet character; the energies will be approximately

$$E_{B_{2u}} = A - G^2\delta'^2\left(\frac{1}{C-A} + \frac{1}{F-A} - \frac{2|G|}{(C-A)(F-A)}\right) \tag{15}$$

and

$$E_{B_{3u}} = A - G^2\delta'^2\left(\frac{1}{D-A} + \frac{1}{E-A} - \frac{2|G|}{(D-A)(E-A)}\right). \tag{16}$$

Analysis of these equations leads to several results. The lowest state will be A_u, since its energy denominators $(C-A, E-A)$ are smaller than those appearing in the B's. Transitions from this level to the ground state will be forbidden in the static lattice, since it contains no singlet character.

The splitting between the other two levels derived from ${}^3Z_2$ will be smaller because the average energy denominators are the same for both. The lower state will be the one with the smallest energy denominator; if $C-A < E-A$, the state derived from ${}^3Z_3$ will be lower, while if $C-A > E-A$, that derived from ${}^3Z_1$ will be lower. In thermal equilibrium the lower state will be preferentially populated, hence the zero-field polarization of the luminescence will tend to reflect the character of this state. One feature of this is that if the zero-order "X" states are lower than the "Y," the luminescence will be "Y" polarized, and vice versa. This is because the state which primarily determines the energy is the triplet X or Y, while that which determines the polarization is the singlet. Since the ${}^3X$ and ${}^1Y$ occur in one block, and ${}^3Y$ and ${}^1X$ in another, the level whose energy is primarily determined by ${}^3X$ will emit Y light, and vice versa. These conclusions will not necessarily apply in the absence of thermal equilibrium, however.

One finds explicitly that, in the perturbation expression, the splitting between B_{2u} and A_u is given by

$$E_{B_{2u}} - E_{A_u} = G^2\delta'^2 \frac{F-E}{(F-A)(E-A)}\left(1 - \frac{2|G|}{C-A}\right). \tag{17}$$

But $F-E$ is just the exchange splitting, so one can write, approximately,

$$E_{B_{2u}} - E_{A_u} \propto (\text{exchange}) \times (\text{spin orbit})^2 . \tag{18}$$

Similarly, one finds that the splitting between the B_u's goes approximately as

$$E_{B_{3u}} - E_{B_{2u}} \propto (\text{exchange}) \times (\text{spin orbit})^2 \times (\text{crystal-field splitting}) , \tag{19}$$

where the crystal-field splitting is the zero-order difference in energy between X and Y levels (and is zero in the simple cubic cesium halides). If one relates this to the differences in g factors of the V_K center, one finds

$$E_{B_{3u}} - E_{B_{2u}} \propto (\text{exchange}) \times (\text{spin-orbit}) \times (g_y - g_x). \tag{20}$$

Qualitative analysis of the effect of an applied magnetic field is somewhat involved, but some insight into admixtures with the A_u state may be obtained. In particular, although a magnetic field along the center axis (i.e., z'-direction) will not mix any singlet into A_u, a field with components perpendicular to the axis wall. For example, $H_{x'}$ will mix together ${}^1X$ and ${}^3Z_2$.

Since none of the centers studied in early experiments on the fcc alkali halides[5] were parallel to $\vec{H}$, the applied field will admix singlet into A_u for all of the centers. Consequently, the A_u level will play a significant role in the field dependence of the luminescence. The cesium halides are of particular interest because when the crystal is oriented [001], one of the three centers will be oriented parallel to $\vec{H}$. In this case, the A_u level will be unaffected by $\vec{H}$ and will not be a source of luminescence. Because the initially degenerate B levels are split apart by $\vec{H}$, there exists the possibility that one will cross A_u. Furthermore, polarization effects will be strictly determined by the relative populations of the B levels.

III. CALCULATIONS

A. KI

Potassium iodide is a good system to consider, because its variation of decay time with temperature has been thoroughly studied and decay parameters have been inferred.[23] Furthermore, its V_K parameters have been measured,[16] providing fairly good initial estimates of many of the parameters.

Fischbach *et al.*[23] analyzed in detail the variations of intensities and lifetimes in the 3.3-eV band as a function of temperature. The presence of two distinct decay components suggested that the system is not in thermal equilibrium at low temperatures. They used two-level kinetics, treating the two B_u states as degenerate, with equations similar to our Eqs. (8) and (9). Excellent fits to the data were obtained, with the splitting between A and B states ~ 0.69 meV.

In the present case we have applied the three-level kinetics introduced in Sec. II. It seems noteworthy that, using Schoemaker's parameters (Table III) along with an exchange energy[23] of 0.044 eV, we obtain, upon solving the Hamiltonian matrix, an $A-B$ splitting of ~ 0.68 meV. This value of exchange energy is very close to that deduced in absorption by Petroff *et al.*,[14] and although it may be fortuitous that the same value appears appropriate for emission, the good value of $A-B$ splitting obtained from it is encouraging.

We find that in the three-level scheme good, though not necessarily optimum, zero-field lifetimes versus temperature values are obtained with τ_{1R} infinite, τ_{2R} and τ_{3R} each equal to 1.07 μsec, and τ_{12} equal to 0.94 μsec. The tunneling terms are omitted. It should be noted that above about 5 °K we predict two "fast" lifetime components. However, their lifetimes are within ~ 0.1 μsec of one another, and it is doubtful whether they can be experimentally resolved. We also calculate the experimentally observed result, that the intensity of the fast component decreases with increasing temperature.

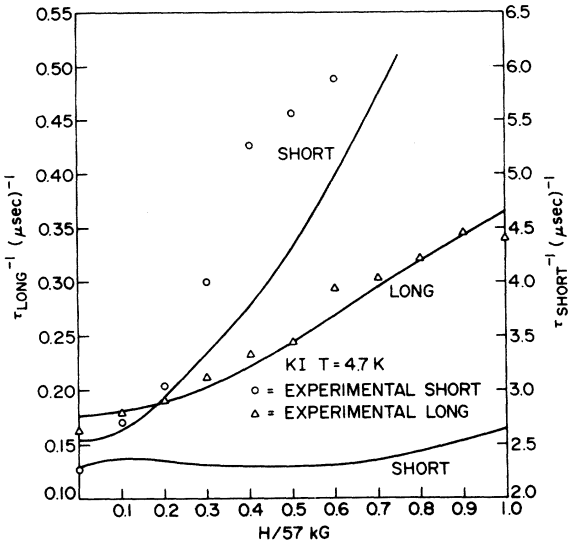

FIG. 1. Reciprocal lifetimes τ^{-1} vs applied magnetic field H for the 3.3-eV luminescence in KI at 4.7 °K. Theoretical results are shown as solid lines.

With the above parameters, we then computed lifetimes, polarizations, and relative intensities for several combinations of magnetic field and temperature. Results are shown in Figs. 1–3.

Figure 1 illustrates the theoretical and experimental variation of lifetimes versus H, at 4.7 °K. Only theoretical results for the [101] centers are given; there are also three lifetime components for the [110] centers, but for large H we predict that the intensity from these centers will be weak, and it has not been identified experimentally. The lower of the two "short" components shown theoretically has not been observed either. Agreement for the components shown is satisfactory. The variation of the upper short lifetime with H is rather sensitive to the nonradiative coupling between the B_{2u} and B_{3u} states; we have assumed them to be coupled by the same one-phonon mechanism which couples the A_u to the B_u states.

Figure 2 indicates the variation of circular polarization with T^{-1}, at $H=57$ kG. In both Figs. 2 and 3, both theoretical and experimental polarizations are normalized to one at maximum values of the variables. Also shown is the predicted luminescence intensity versus T^{-1}. Agreement with experiment is fair.

Figure 3 shows computed circular polarizations and luminescence intensities as functions of H, for $T=4.7$ °K. Also shown are some experimental polarizations and intensities. Agreement is quite good. Taken all together, comparison of our KI results with experiment is quite good and suggests not only that the luminescence occurs from non-

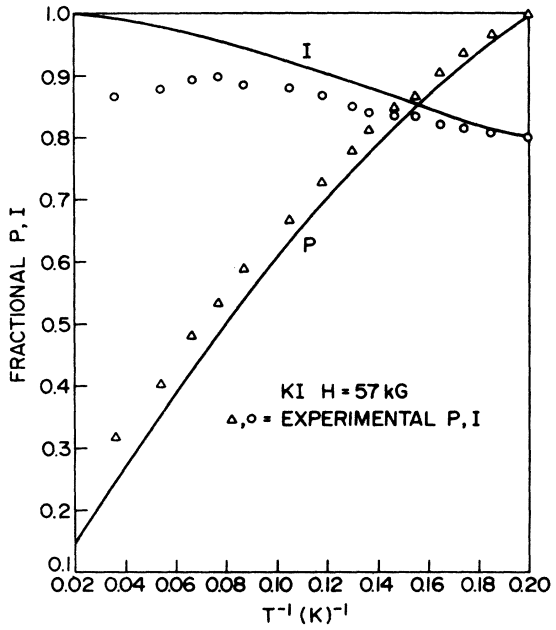

FIG. 2. Fractional circular polarization P and luminescence intensity I vs reciprocal temperature for the 3.3-eV luminescence in KI with an applied magnetic field of 57 kG. Theoretical results are shown as solid lines.

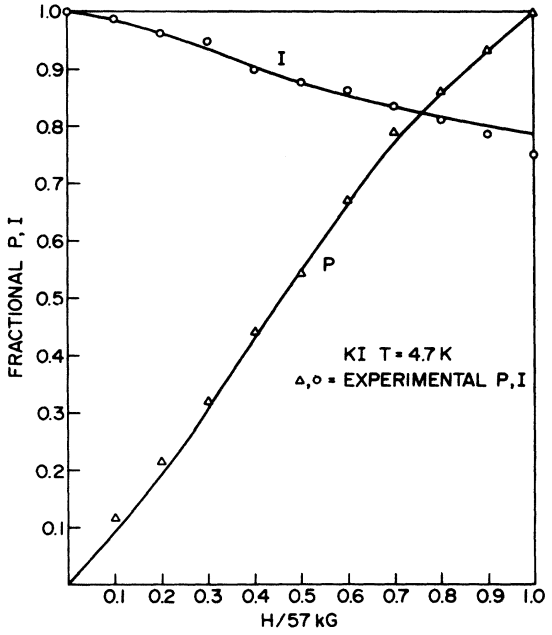

FIG. 3. Fractional circular polarization P and luminescence intensity I vs applied magnetic field H for the 3.3-eV luminescence in KI at 4.7 °K. Theoretical results are shown as solid lines.

equilibrium triplets, but that estimates of the exciton parameters are probably rather reliable.

B. CsI

It is reasonable to consider the 3.65-eV STE emission in CsI to correspond to the 3.3-eV emission in KI. The temperature dependence of the lifetime of the 3.65-eV emission has been measured and analyzed by Lamatsch *et al.*[24] They fitted their data by a two-level model in which both levels were in thermal equilibrium at all temperatures. The two levels were separated by ~2 meV, and the lower level had a long (but finite) radiative lifetime.

It has been suggested[23] that their data agree equally well with the simple nonequilibrium model used previously to describe the KI lifetime data in the absence of an applied field. This approach has further advantages, one of which is the capability of explaining a weak fast decay component (lifetime $\lesssim 1$ μsec) which was observed but which was not accounted for the equilibrium model. Independent of this choice, the ~2-meV activation energy is most simply interpreted as the $E_u - A_{1u}$ zero-field splitting, corresponding to the $B_{2u} - A_u$ and $B_{3u} - A_u$ splittings for KI. However, as will be seen, this magnitude is so large as to be evidently inconsistent with the compelling evidence of level crossing at ~45 kG.

Measurements of radiative lifetimes and circular polarizations under an applied magnetic field have led to striking results for CsI crystals with a [001] axis parallel to the field.[7] Figure 4 shows the lifetimes versus field at 4.7 °K for the long-lived component, which separates into two in this orientation. Figure 5 shows circular polarization versus H at 4.6 °K. Theoretical results, to be discussed later, are also shown. It is noteworthy that both polarization and one lifetime component have extrema at ~45 kG, that polarization versus

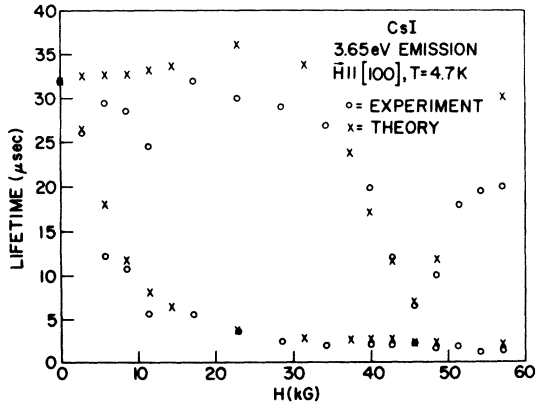

FIG. 4. Lifetime vs applied magnetic field H for the 3.65-eV luminescence in CsI at 4.7 °K. Crystal orientation [001].

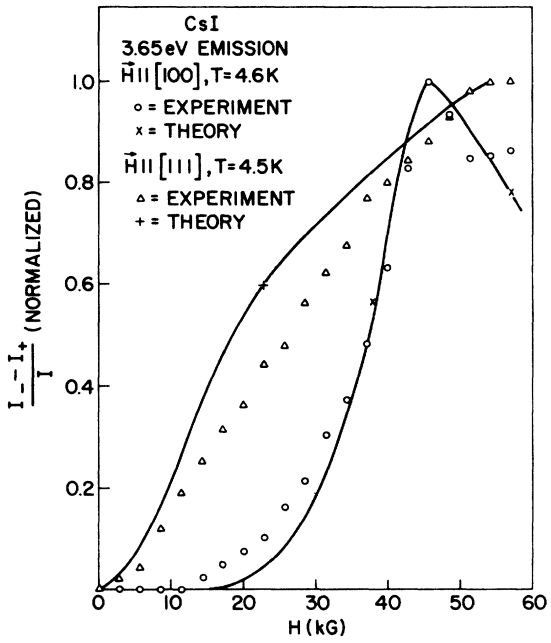

FIG. 5. Fractional circular polarization vs applied magnetic field H for the 3.65-eV luminescence in CsI. Results are given for both [001] and [111] crystal orientations. Theoretical results are shown as solid lines.

H increases very slowly for small H, and that the second component of the lifetime falls monotonically with increasing H.

As mentioned in Sec. II, a [001] CsI crystal will have one of three centers aligned parallel to H, and two aligned perpendicular to H. In the former case the lowest triplet level is unaffected by H, while the upper two (initially degenerate) are split apart. Thus there is the possibility of level crossing. It is suggestive to attribute the features at 45 kG to level crossing; our calculations (or simple perturbation theory) then indicate, however, that the zero-field splitting is only ~0.5 meV if $g=2$, considerably smaller than the 2 meV deduced from zero-field temperature-dependent lifetime measurements.

The small variation of polarization with H for small H suggests that the populations of the upper two triplet levels are approximately independent of H, for small H and at 4.5 °K. The one-phonon radiationless transition probability introduced in Sec. IIE has a maximum value at 4.5 °K for an energy of ~0.65 meV. If the upper two levels were not coupled to each other, radiationless transitions from the lowest state to the upper states might be expected to govern the polarization, and one would expect polarization versus H to be weakly varying if the zero-field splitting were ~0.65 meV. This is fairly close to ~0.5 meV, but it should be noted that were the commonly quoted radiationless transition probability (which varies as $|E_j - E_i|^3$, rather than $|E_j - E_i|^2$) used, the maximum would be at ~1.2 meV.

Thus at the outset one is faced with several choices for the zero-field splitting. For reasons to be discussed later, we assumed that ~0.5 meV is the proper value and applied the techniques of Sec. II to compute experimental quantities. V_K data are not available for CsI, but estimates of parameters may be made from the KI results. Furthermore, we are unable to use the zero-field lifetime data as a guide to the various τ's. Thus the values which we have chosen as best fits to H-field data are not subject to the same independent evaluation as in KI.

In order that the lifetime shorten rapidly as the levels cross, another relaxation mechanism must be involved. When levels are close to each other the one-phonon transition probability becomes very small, and the Orbach process using the third level is not sufficient to account for the singular behavior. However, a no-phonon tunneling between levels is possible, as given in Eq. (9), and we have fit the parameters τ_T and A_T to the lifetime variation around 45 kG. We assume that the same mechanism and the same values govern transitions between the upper two levels near $H=0$, although this does not have a large effect on the results. As mentioned earlier, the depopulation of the metastable level near the crossing may also be a radiative process arising from high-order hyperfine interactions.

The results presented here were obtained with the values of parameters given in Table III. These parameters lead to a zero-field splitting between the lowest and the upper two triplets of 0.52 meV. The other parameter values are τ_{1R} infinite, $\tau_{2R} = \tau_{3R} = 0.7$ μsec, $\tau_{12} = 23.6$ μsec, $\tau_T = 7$ μsec, $A_T = 18350.$ eV^{-1}. For all centers the initial populations of all three states are chosen equal. Both theoretical and experimental polarizations are normalized to 1 at appropriate values of H.

Figures 5 and 6 show experimental and theoretical polarizations and lifetimes versus H for the [111] crystal. Agreement is quite good in the case of the lifetimes, not as good in the case of the polarizations.

Although a fairly good fit to experimental data for both crystal orientations has been made, the many parameters used raises the question of how significant the fit is. This is especially important in view of the question of zero-field splittings, as mentioned. We attempted to fit the data with zero-field splittings of various values and were generally unsuccessful. With a zero-field splitting of ~2 meV *and* a large g value, it was possible to reduce the lifetimes from ~32 μsec at zero field to

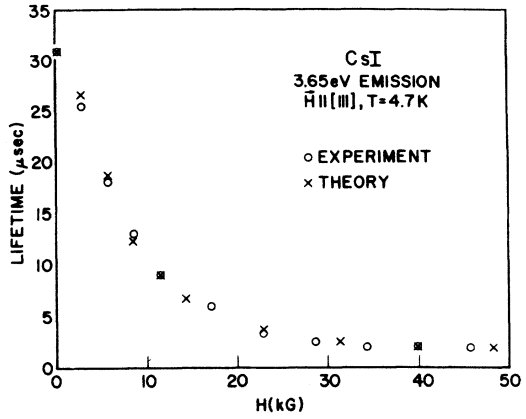

FIG. 6. Lifetime vs applied magnetic field H for the 3.65-eV luminescence in CsI at 4.7 °K. Crystal orientation [111].

~6 μsec at ~45 kG. However, the variation with field was much too smooth as compared with the rather abrupt variation observed experimentally. Furthermore, it is difficult to obtain good agreement with the polarization data. We are forced to conclude that the temperature dependence measured by Lamatsch *et al.*[24] arises from another mechanism such as the Raman effect or phonon-assisted transitions.

With a zero-field splitting of ~1.2 meV and radiationless transition probabilities varying as the cube of energy differences, it was possible to obtain fairly good variation of polarization with field. However, the variation of lifetime with field could not be easily reproduced; unless the g value were ~2.5 times the value computed, there would be no level crossing and no "resonant" behavior.

Thus, over all, the zero-field splitting of ~0.5 meV seems most likely. With such a splitting a level-crossing resonance occurs for the [001] center, and by including tunneling one can obtain very good agreement with lifetime data. Polarization data are more difficult to fit, however. If the states have equal initial populations, polarization is largely determined by the differential radiationless transition rates from the lowest state to the upper two. With a zero-field splitting as small as 0.52 meV and a radiationless transition probability varying as the cube of energy differences, population of the highest state is favored and the polarization is large and negative for small and moderate H, eventually becoming positive. This is not in agreement with experiment. But fairly good results are obtained from an E^2 variation, as indicated. Investigation of the theory[20] indicates that an E^2 variation comes from the Debye density of phonon states, and an additional factor of E comes from the one-phonon transition matrix. However, this result is valid only for long-wavelength unperturbed phonons. The present situation involves perturbed "local" phonons with vibrational amplitudes which vary rapidly with distance around the center. Hence there is no clear theoretical guide as to the variation of transition probability with energy, so we chose one which seems to give fairly good results.

Several other experimental features which are consistent with the theory should be pointed out. First, both experimentally and theoretically the smoothly varying lifetime component falls off more rapidly with H for the [001] crystal than for the [111] crystal. Second, the polarization curve for the [111] crystal tends to lie above that of the [001] crystal. This occurs because the lowest level of the STE in the [111] crystal acquires some singlet character in the external field, and the polarization associated with this is added to the nearly cancelling contributions from the upper two levels. For the [001] center in the [001] crystal only the upper two levels participate.

Despite some questions of detail, it appears that the triplet model of the STE, with nonequilibrium distributions, describes well the 3.65-eV luminescence of CsI.

IV. CONCLUSIONS

The model developed in this paper has been applied with reasonable success to describe the triplet self-trapped exciton luminescence in KI and CsI. It is expected that other alkali-halide excitons can be treated in a similar fashion. In addition, the theory can be applied to Jahn-Teller distorted (sp) systems[4,6] and to the triplet states of the M center, with some modifications, provided that accurate estimates of the parameters can be made.

ACKNOWLEDGMENT

We gratefully acknowledge preprints from Dirk Schoemaker, who supplied V_K-center parameters as well as ideas about angular momentum quenching.

*Research supported in part by the Office of Naval Research Contract No. USN-ONR-N00014-67A-0370.

[1]A. Fukuda, Phys. Rev. B **1**, 4161 (1970).
[2]R. S. Knox, *Theory of Excitons* (Academic, New York, 1963).
[3]M. N. Kabler, Phys. Rev. **136**, A1296 (1964).
[4]P. Edel, C. Hennies, Y. Merle D'Aubigne, R. Romestain, and Y. Twarowski, Phys. Rev. Lett. **28**, 1268 (1972).
[5]M. J. Marrone and M. N. Kabler, Phys. Rev. Lett. **27**, 1283 (1971).
[6]A. Fukuda and P. Yuster, Phys. Rev. Lett. **28**, 1032 (1972).

[7]M. N. Kabler, M. J. Marrone, and W. B. Fowler, Izv. Akad. Nauk SSSR Ser. Fiz. 37, 341 (1973). The same article appears in *Luminescence of Crystals, Molecules and Solutions*, edited by F. Williams (Plenum, New York, 1973).

[8]E. U. Condon and G. H. Shortley, *Theory of Atomic Spectra* (Cambridge U. P., London, 1935).

[9]W. B. Fowler, Phys. Status Solidi **33**, 763 (1969).

[10]See, e.g., L. I. Schiff, *Quantum Mechanics*, 2nd ed. (McGraw-Hill, New York, 1955), p. 233.

[11]C. J. Ballhausen and H. B. Gray, *Molecular Orbital Theory* (Benjamin, New York, 1965).

[12]This point has been clearly made by Schoemaker (Ref. 16), and we use his notation and some of his results in the following. However, our x and y axes are opposite to Schoemaker's.

[13]Y. Onodera and Y. Toyozawa, J. Phys. Soc. Jap. **22**, 833 (1967); T. Miyata and T. Tomiki, J. Phys. Soc. Jap. **24**, 1286 (1968).

[14]Y. Petroff, R. Pinchaux, C. Chekroun, M. Balkanski, and H. Kamimura, Phys. Rev. Lett. **27**, 1377 (1971).

[15]M.J. Marrone, F. W. Patten, and M. N. Kabler, Phys, Rev. Lett. 31 467 (1973).

[16]D. Schoemaker, Phys. Rev. B **7**, 786 (1973).

[17]Because the free-electron g value is 2.0023, not 2.0, a slight adjustment must be made before experimental and theoretical values are compared.

[18]T. G. Castner and W. Känzig, Phys. Chem. Solids **3**, 178 (1957).

[19]R. G. Fuller, R. T. Williams, and M. N. Kabler, Phys. Rev. Lett. **25**, 446 (1970); R. T. Williams and M. N. Kabler (unpublished).

[20]See, e.g., P. L. Scott and C. D. Jeffries, Phys. Rev. **127**, 32 (1962).

[21]W. Siebrand, J. Chem. Phys. **46**, 440 (1967).

[22]R. Orbach, Proc. R. Soc. A **264**, 456 (1961).

[23]J. U. Fischbach, D. Fröhlich, and M. N. Kabler, J. Lumin. **6**, 29 (1973).

[24]H. Lamatsch, J. Rossel, and E. Saurer, Phys. Status Solidi B **48**, 311 (1971).